J Oceanogr (2011) 67:219–230
DOI 10.1007/s10872-011-0019-2

ORIGINAL ARTICLE

Maximum angle method for determining mixed layer depth from seaglider data

Peter C. Chu · Chenwu Fan

Received: 19 August 2010 / Revised: 29 November 2010 / Accepted: 7 March 2011 / Published online: 1 April 2011

Abstract A new maximum angle method has been developed to determine surface mixed-layer (a general name for isothermal/constant-density layer) depth from profile data. It has three steps: (1) fitting the profile data with a first vector (pointing downward) from an upper level to a depth and a second vector (pointing downward) from that depth to a deeper level; (2) identifying the angle (varying with depth) between the two vectors; (3) after fitting and calculating angle all depths, and then selecting the depth with maximum angle as the mixed layer depth (MLD). Temperature and potential density profiles collected from two seagliders in the Gulf Stream near the Florida coast during 14 November–5 December 2007 were used to demonstrate the method's capability. The quality index (1.0 for perfect identification of the MLD) of the maximum angle method is about 0.96. The isothermal layer depth is generally larger than the constant-density layer depth, i.e., the barrier layer occurs during the study period. Comparison with the existing difference, gradient, and curvature criteria shows the advantage of using the maximum angle method. Uncertainty in determining MLD because of varying threshold using the difference method is also presented.

Keywords Ocean mixed layer depth · Isothermal layer · Constant density layer · Barrier layer · Maximum angle method · Optimal linear fitting · Difference criterion · Gradient criterion · Curvature method

P. C. Chu (✉) · C. Fan
Department of Oceanography, Naval Postgraduate School, Monterey, CA 93940, USA
e-mail: pcchu@nps.edu
URL: http://faculty.nps.edu/pcchu

1 Introduction

Transfer of mass, momentum, and energy across the bases of surface isothermal and constant-density layers provides the source for almost all oceanic motions. Underneath the surface constant-density and isothermal layers, there exist layers with strong vertical gradients such as the pycnocline and thermocline. The mixed layer depth (MLD) (a general name for isothermal/constant-density layer depth) is an important parameter which influences the evolution of the sea surface temperature. The isothermal layer depth (H_T) is not necessarily identical to the constant-density layer depth (H_D) because of salinity stratification. There are areas of the World Ocean where H_T is deeper than H_D (Chu et al. 2002). The difference between H_D and H_T is defined as the barrier layer. The barrier layer thickness (BLT) is often referred to as the difference, $\mathrm{BLT} = H_T - H_D$. For example, a barrier layer was observed from a seaglider in the western North Atlantic Ocean near the Florida coast (30.236°N, 78.092°W) at GMT 23:20 on 19 November 2007 (Fig. 1).

Objective and accurate identification of H_T and H_D is important for the determination of barrier layer occurrence and its climate impact. Three types of criteria (difference, gradient, and curvature) are available for identifying H_T from profiling data. The difference criterion requires the deviation of T (or ρ) from its near-surface (i.e., reference level) value to be smaller than a certain fixed value. The gradient criterion requires $\partial T/\partial z$ (or $\partial \rho/\partial z$) to be smaller than a certain fixed value. The curvature criterion requires $\partial^2 T/\partial z^2$ (or $\partial^2 \rho/\partial z^2$) to be maximum at the base of the mixed layer ($z = -H_D$).

The difference and gradient criteria are subjective because there is no objective way to determine the criteria. For example, the criterion for determining H_T for

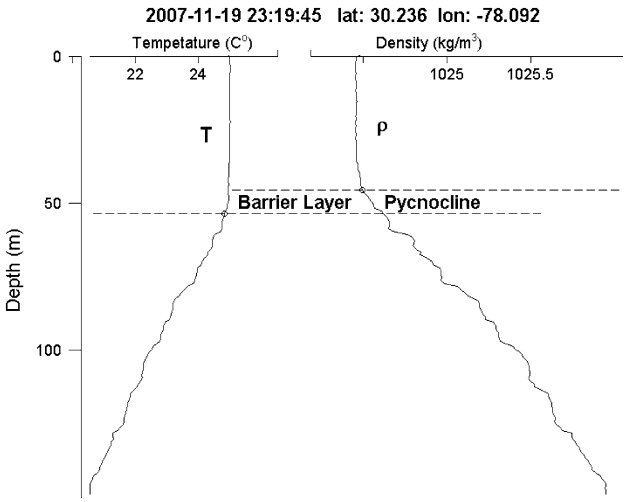

Fig. 1 Isothermal, constant-density, and barrier layers were observed by a seaglider in the western North Atlantic Ocean near the Florida coast (30.236°N, 78.092°W) at GMT 23:20 on 19 November 2007

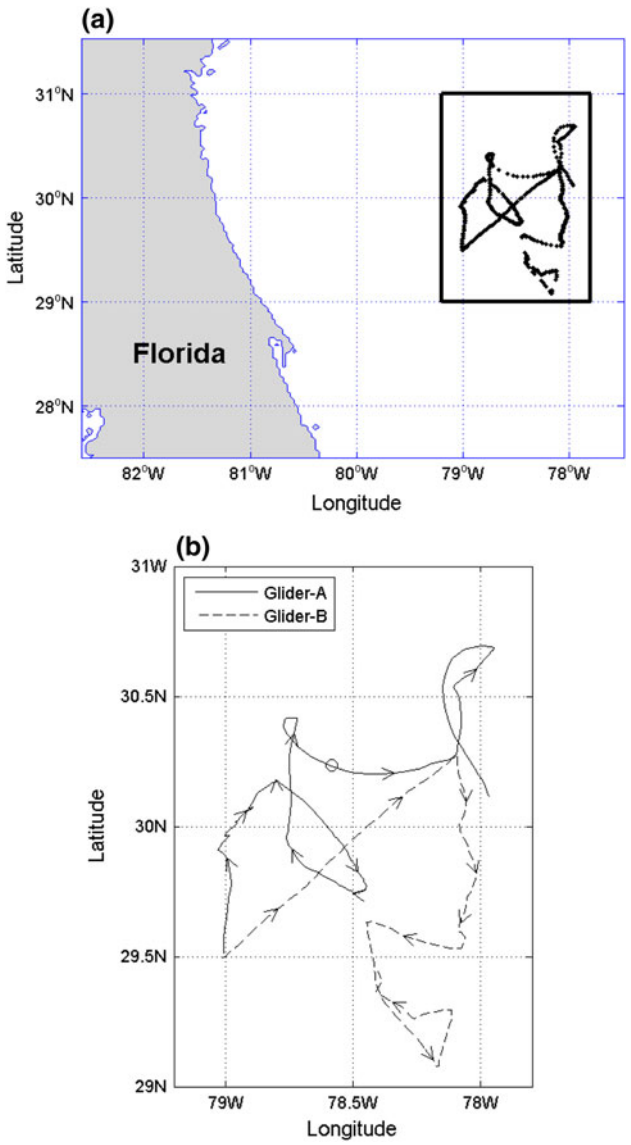

Fig. 2 **a** Location of the glider data, and **b** drifting paths of two gliders with the station marked by a *circle* for demonstration

temperature varies from 0.8°C (Kara et al. 2000), 0.5°C (Wyrtki 1964) to 0.2°C (de Boyer Montegut et al. 2004). The reference level changes from near surface (Wyrtki 1964) to 10-m depth (de Boyer Montegut et al. 2004). The criterion for determining H_D for potential density varies from 0.03 kg/m^3 (de Boyer Montegut et al. 2004), 0.05 kg/m^3 (Brainerd and Gregg 1995), to 0.125 kg/m^3 (Suga et al. 2004). The curvature criterion is an objective method (Chu et al. 1997, 1999, 2000; Lorbacher et al. 2006), but is hard to use for profile data with noise (even small), which will be explained in Sect. 5. Thus, it is urgent to develop a simple objective method for determining MLD with the capability of handling noisy data.

In this study, a new maximum angle method has been developed to determine H_T and H_D and the gradients of the thermocline and pycnocline. The method was tested using profiles collected by two seagliders of the Naval Oceanographic Office in the Gulf Stream region near the Florida coast during 14 November–5 December 2007. The maximum angle method is compared with the existing methods. The results demonstrate its capability. The outline of this paper is as follows. Section 2 describes hydrographic data from the two seagliders. Section 3 presents the methodology. Sections 4 and 5 compare the maximum angle method with the existing methods. Section 6 shows the occurrence of barrier layer from this dataset. Section 7 presents the conclusions.

2 Seaglider data

Two seagliders were deployed in the Gulf Stream region near the Florida coast by the Naval Oceanographic Office (Mahoney et al. 2009) from two nearby locations on 14 November 2007 with one at (79.0°W, 29.5°N) (Seaglider-A) and the other at (79.0°W, 29.6°N) (Seaglider-B) (Fig. 2). They encountered some eddies.

The seaglider goes up and down in an oblique direction, not vertically. Data collected during a downward-upward cycle are divided into two parts, with the first one from the surface to the deepest level and the second one from the deepest level to the surface. Each part represents an individual profile with the averaged longitude and latitude of the data points as the horizontal location. These temperature and potential density profiles go through a series of quality control checks: min–max check (e.g., disregarding any temperature data <-2 and >35°C), error anomaly check (e.g., rejecting temperature and salinity data

deviating more than 3 standard deviations from climatology), seaglider-tracking algorithm (screening out data with obvious seaglider position errors), max-number limit (limiting a maximum number of observations within a specified and rarely exceeded space–time window), and buddy check (tossing out contradicting data). The climatological data set used for the quality control is the Navy's generalized digital environmental model (GDEM) climatological temperature and salinity data set. After the quality control, 514 profiles of (T, ρ) are available with 265 profiles from Seaglider-A and 249 profiles from Seaglider-B. The vertical resolution of the profile varies from less than 1 m for upper 10 m to approximately 1–3 m below 10-m depth. All the profiles are deeper than 700 m and exhibit layered structure: isothermal (constant-density) layer, thermocline (pycnocline), and deep layer.

3 Determination of (H_T, H_D)

Let the potential density and temperature profiles be represented by [$\rho(z_k)$, $T(z_k)$]. Here, k increases downward with $k = 1$ at the surface or nearest to the surface and K the total number of the data points for the profile. The potential density profile is taken for illustration of the new methodology. The depths corresponding to $\rho_{\min}$ and $\rho_{\max}$, $z_{\min}$ and $z_{\max}$, respectively, are found. Without noise, $z_{\min}$ should be z_1 and $z_{\max}$ should be z_K. The vertical density difference, $\Delta\rho = \rho_{\max} - \rho_{\min}$, represents the total variability of potential density. Theoretically, the variability is 0 in the constant-density layer and large in the pycnocline beneath the mixed layer. It is reasonable to identify the main part of the pycnocline between the two depths: $z_{(0.1)}$ and $z_{(0.7)}$, with the difference to $\rho_{\min}$ as $0.1\Delta\rho$ and $0.7\Delta\rho$ (Fig. 3), respectively. Let n be the number of data points between $z_{(0.1)}$ and $z_{(0.7)}$ and $m = \min(n, 20)$.

Figure 4 is a schematic of the method's vector fitting. At depth z_k (marked by a circle in Fig. 4), a first vector ($\mathbf{A}_1$, downward positive) is constructed with linear polynomial fitting of the profile data from z_{k-j} to z_k with

$$j = \begin{cases} k-1, & \text{for} \quad k \le m \\ m, & \text{for} \quad k > m \end{cases}. \tag{1}$$

A second vector ($\mathbf{A}_2$, pointing downward) from one point below that depth (i.e., z_{k+1}) is constructed to a deeper z_{k+m}. The dual-linear fitting (Chu and Fan 2010) can be represented by

$$\rho(z) = \begin{cases} c_k^{(1)} + G_k^{(1)} z, & z = z_{k-j}, z_{k-j+1}, \ldots, z_k \\ c_k^{(2)} + G_k^{(2)} z, & z = z_{k+1}, \ldots, z_{k+m} \end{cases}, \tag{2}$$

where $c_k^{(1)}, c_k^{(2)}, G_k^{(1)}, G_k^{(2)}$ are the fitting coefficients.

At the constant-density (isothermal) layer depth, the angle θ_k reaches its maximum value (see Fig. 4b), and

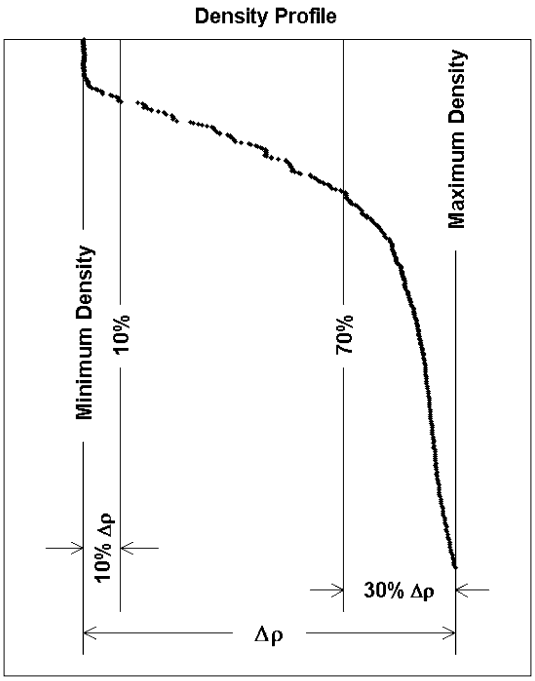

Fig. 3 Illustration for determination of $z_{(0.1)}$ and $z_{(07)}$. There are n data points between $z_{(0.1)}$ and $z_{(07)}$

smaller if z_k is inside (Fig. 4a) or outside (Fig. 4c) of the mixed layer. Thus, the maximum angle principle can be used to determine the mixed (or isothermal) layer depth,

$$\theta_k \to \max, \quad H_D = -z_k.$$

In practice, the angle θ_k is hard to calculate, so $\tan\theta_k$ is used instead, i.e.,

$$\tan\theta_k \to \max, \quad H_D = -z_k, \quad G^{(1)} = G_k^{(1)}, \quad G^{(2)} = G_k^{(2)}, \tag{3}$$

where $G^{(1)} \approx 0$ is the vertical gradient in the mixed layer, and $G^{(2)}$ is the vertical gradient in the thermocline (pycnocline). With the given fitting coefficients $G_k^{(1)}, G_k^{(2)}$, $\tan\theta_k$ can be easily calculated by

$$\tan\theta_k = \frac{G_k^{(2)} - G_k^{(1)}}{1 + G_k^{(1)} G_k^{(2)}}. \tag{4}$$

The maximum angle method [i.e., Eqs. (1)–(4)] was used to calculate H_T and H_D from 514 pairs of temperature and potential density profiles from the two seagliders. With high vertical resolution of the data, H_T and H_D can be determined for all profiles. The potential density profile at the station (shown in Fig. 1) located at (30.236°N, 78.092°W) is taken as an example for illustration (Fig. 5a). At $z = -H_D$, $\tan\theta_k$ has maximum value (Fig. 5b).

Unlike the existing methods, the maximum angle method not only uses the main feature (vertically uniform) of the mixed layer such as in the difference and gradient

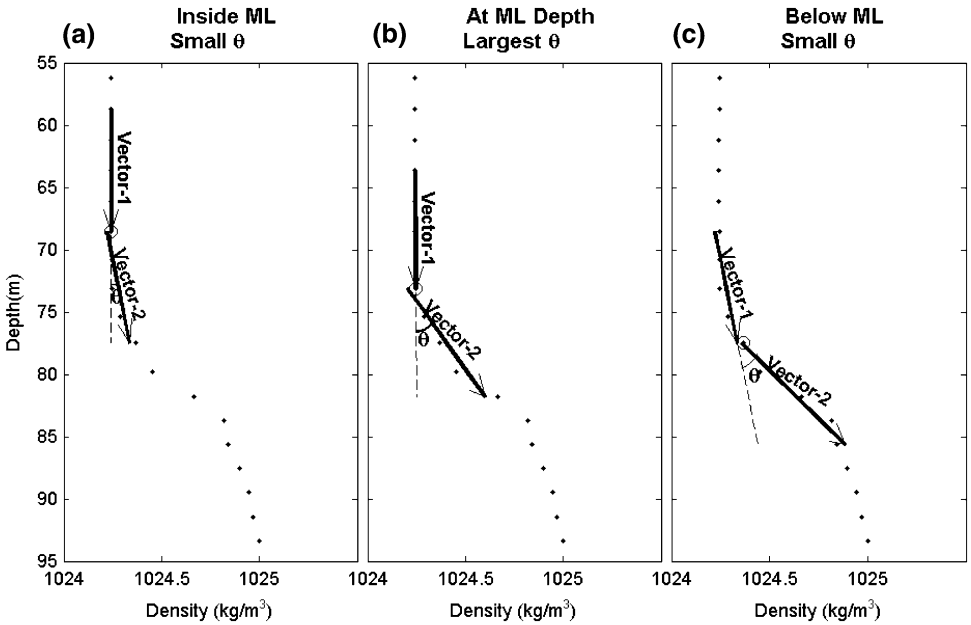

Fig. 4 Illustration of the method: **a** z_k is inside the mixed layer (small θ), **b** z_k at the mixed layer depth (largest θ), and **c** z_k below the mixed layer depth (small θ)

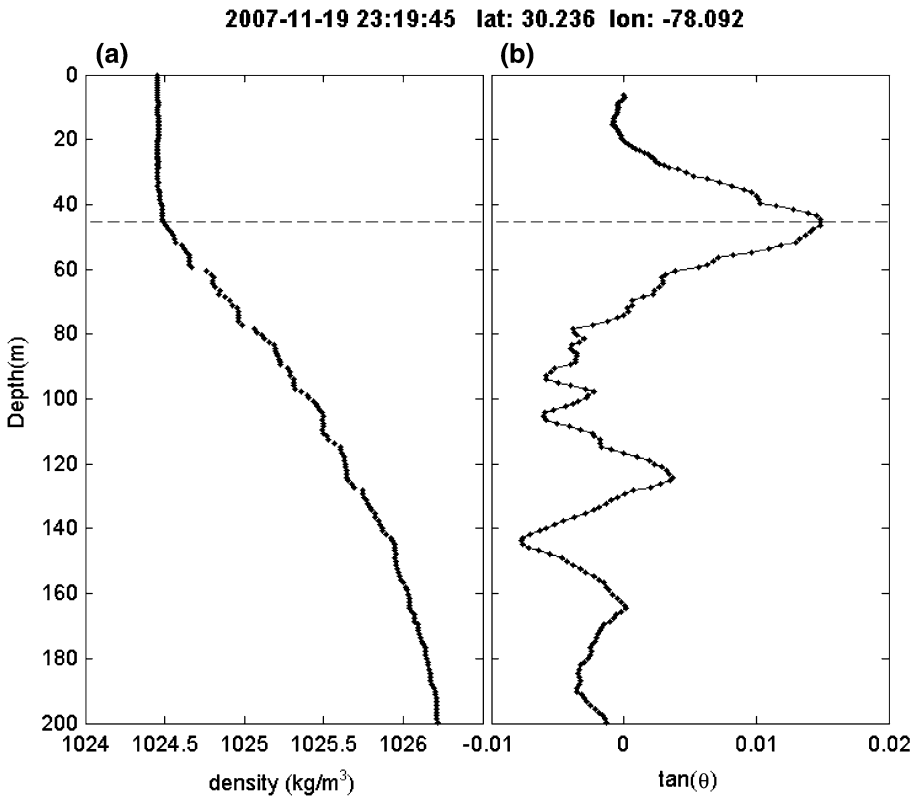

Fig. 5 Determination of H_D using the maximum angle method: **a** density profile at the seaglider station (shown in Fig. 1) located at (30.236°N, 78.092°W) at GMT 23:20 on 19 November 2007, and **b** calculated tan θ_k. It is noted that the depth of the maximum tan θ_k corresponds to the mixed layer depth and only the upper part of the potential density profile is shown here

criteria, but also uses the main characteristics in the pycnocline (sharp gradient) beneath the mixed layer (see Fig. 3). After MLD is determined, the vertical gradient of the thermocline (pycnocline), $G^{(2)}$, is also calculated. A disadvantage of the maximum angle method is its use of two linear regressions [see Eq. (2)]. Reliable regression needs a sufficient sample size. For profiles with very few data points (low resolution), the maximum angle method might not work. The seaglider data described in Sect. 2 are high-resolution profiles, and therefore are perfect for

testing the maximum angle method through comparison with the existing methods. Large gradients often occur in the near-surface layer (within 10 m), which leads to falsely shallow MLDs using the gradient method (i.e., the gradient method performs much worse). Therefore, the maximum angle method is compared with the threshold and curvature methods in next two sections.

4 Comparison between maximum angle and threshold methods

Lorbacher et al. (2006) proposed a quality index (QI)

$$\mathrm{QI} = 1 - \frac{\mathrm{rmsd}(\rho_k - \hat{\rho}_k)|_{(H_1, H_\mathrm{D})}}{\mathrm{rmsd}(\rho_k - \hat{\rho}_k)|_{(H_1, 1.5\times H_\mathrm{D})}}, \quad (5)$$

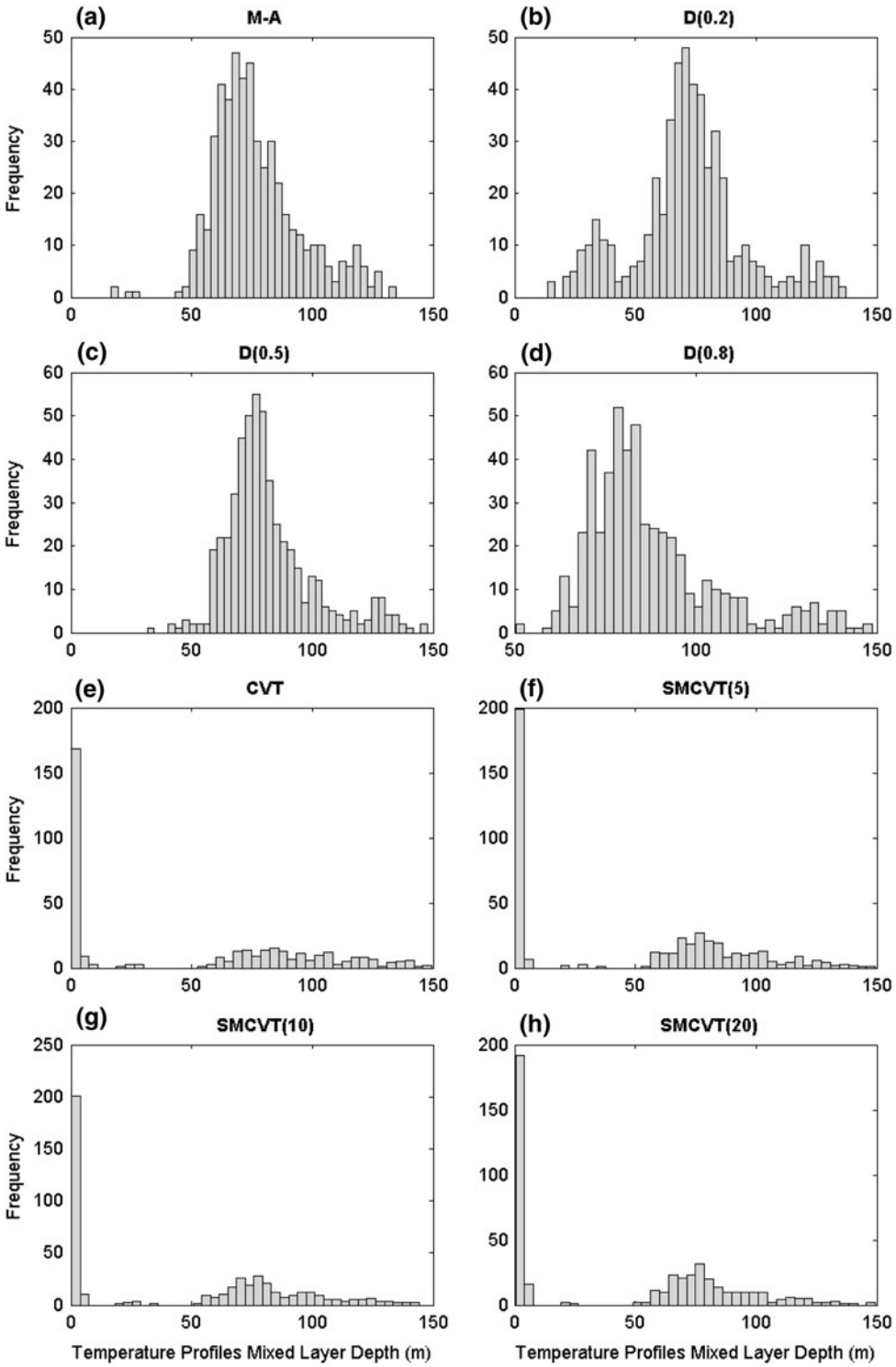

Fig. 6 Histograms of H_T identified using **a** the maximum angle method (M-A) on original profiles, the difference method (D) on original profiles with thresholds of **b** 0.2°C, **c** 0.5°C, **d** 0.8°C, and the curvature method (CVT) on profiles after **e** no, **f** 5 times, **g** 10 times, **h** 20 times 5-point smoothing (SMCVT)

to evaluate various schemes for H_D (or H_T) determination. Here, $\rho_k = \rho(z_k)$ is the observed profile; $\hat{\rho}_k$ = mean potential density between z_1 and $z = -H_D$; and rmsd (x_k, y_k) is the root-mean-square difference between $\{x_k\}$ and $\{y_k\}$. For a perfect identification, $\text{rmsd}(\rho_k - \hat{\rho}_k)|_{(H_1,H_D)} = 0$ and QI = 1. Higher QI values correspond to more reliably identified MLDs. Usually, H_D is defined to be determined with certainty if QI > 0.9; determined with uncertainty if 0.9 > QI > 0.5; and undetermined if QI < 0.5.

Four sets of isothermal depth were obtained from 514 temperature profiles of the two seagliders using the maximum angle method and the threshold method with 0.2°C (de Boyer Montegut et al. 2004), 0.5°C (Monterey and Levitus 1997), and 0.8°C (Kara et al. 2000) thresholds. Figure 6 shows the histograms of 514 H_T values for the four methods. The differences among the three threshold histograms convey the uncertainty of the threshold method. Table 1 shows the statistical characteristics of H_T determined by the four methods. The mean (median) H_T value is 77.2 (73.2) m using the maximum angle method. For the difference method, it increases with the value of the threshold from 71.9 (71.8) m using 0.2°C, to 82.0 (77.9) m using 0.5°C, to 87.6 (82.9) m using 0.8°C.

Obviously, the four histograms show non-Gaussian features. H_T is positively skewed for all the four methods. The skewness of H_T is sensitive to the thresholds: 0.21 using 0.2°C, 1.13 using 0.5°C, and 1.25 using 0.8°C. It is 0.69 using the maximum angle method. The kurtosis of H_T is larger than 3 for all the four methods and sensitive to the thresholds: 3.48 using 0.2°C, 4.46 using 0.5°C, and 4.35 using 0.8°C. It is 3.80 using the maximum angle method.

The histograms of 514 QI values are negatively skewed for the four methods (Fig. 7). Most QI values are larger than 0.980, with a mean value of 0.965 using the maximum angle method (Fig. 7a) and are lower using the threshold method (Fig. 6b–d). The mean QI values for the threshold methods are 0.881 with 0.2°C (Fig. 7b), 0.858 with 0.5°C (Fig. 7c), and 0.833 with 0.8°C (Fig. 7d).

Difference in MLD determination using two thresholds is represented by relative root-mean-square difference (RRMSD),

$$\text{RRMSD} = \frac{1}{\bar{H}^{(1)}}\sqrt{\frac{1}{N}\sum_{i=1}^{N}\left(H_i^{(2)} - H_i^{(1)}\right)^2}, \tag{6}$$

where $N = 514$, is the number of the seaglider profiles; ($H_i^{(1)}$, $H_i^{(2)}$, $i = 1, 2, \ldots, N$) are two sets of MLD identified by the difference method using two different criteria. The RRMSD of H_T is 20.1% between 0.2 and 0.5°C thresholds, 28.5% between 0.2 and 0.8°C thresholds, and 10.0% between 0.5 and 0.8°C thresholds.

Similarly, four sets of constant-density depth were obtained from 514 density profiles of the two seagliders using the maximum angle method and the threshold method with 0.03 kg/m^3 (de Boyer Montegut et al. 2004), 0.05 kg/m^3 (Brainerd and Gregg 1995), and 0.125 kg/m^3 (Monterey and Levitus 1997). Figure 8 shows the histograms of 514 H_D values for the four methods. H_D is positively skewed using the maximum angle method. Difference of the histograms among 0.03 kg/m^3 (Fig. 8b), 0.05 kg/m^3 (Fig. 8c), to 0.125 kg/m^3 (Fig. 8d) threshold implies uncertainty in the difference method. Table 2 shows the statistical characteristics of H_D determined by the four methods. The mean (median) H_D value is 73.2 (70.4) m using the maximum angle method. For the gradient method, it increases with the value of the threshold from 53.3 (60.9) m using 0.03 kg/m^3, to 59.3 (66.2) m using 0.05 kg/m^3, to 68.0 (71.6) m using 0.125 kg/m^3. The skewness of H_D is slightly positive (0.28) using the maximum angle method and slightly negative when it is identified using the threshold method. The negative skewness enhances with the threshold from −0.06 using 0.03 kg/m^3, −0.24 using 0.05 kg/m^3, to −0.59 using 0.125 kg/m^3. The kurtosis of H_D is 4.32 using the maximum angle method and varies with the threshold when the difference method is used. It is 2.37 using 0.03 kg/m^3, 2.74 using 0.05 kg/m^3, and 3.67 using 0.125 kg/m^3.

The histograms of 514 QI values are negatively skewed for the four methods (Fig. 9). Most QI values are larger than 0.980 with a mean value of 0.966 for the maximum angle method (Fig. 9a) and are lower using the threshold method (Fig. 8b–d). The mean QI values are 0.837 with 0.03 kg/m^3 threshold (Fig. 9b), 0.859 with 0.05 kg/m^3 threshold (Fig. 9c), and 0.872 with 0.125 kg/m^3 threshold (Fig. 9d).

Table 1 Statistical characteristics of H_T identified from the two seagliders using the maximum angle, 0.2, 0.5, and 0.8°C thresholds

	Maximum angle	0.2°C threshold	0.5°C threshold	0.8°C threshold
Mean (m)	77.2	71.9	82.0	87.6
Median (m)	73.2	71.8	77.9	82.9
Standard deviation (m)	18.3	23.4	18.4	18.0
Skewness	0.69	0.21	1.13	1.25
Kurtosis	3.80	3.48	4.46	4.35

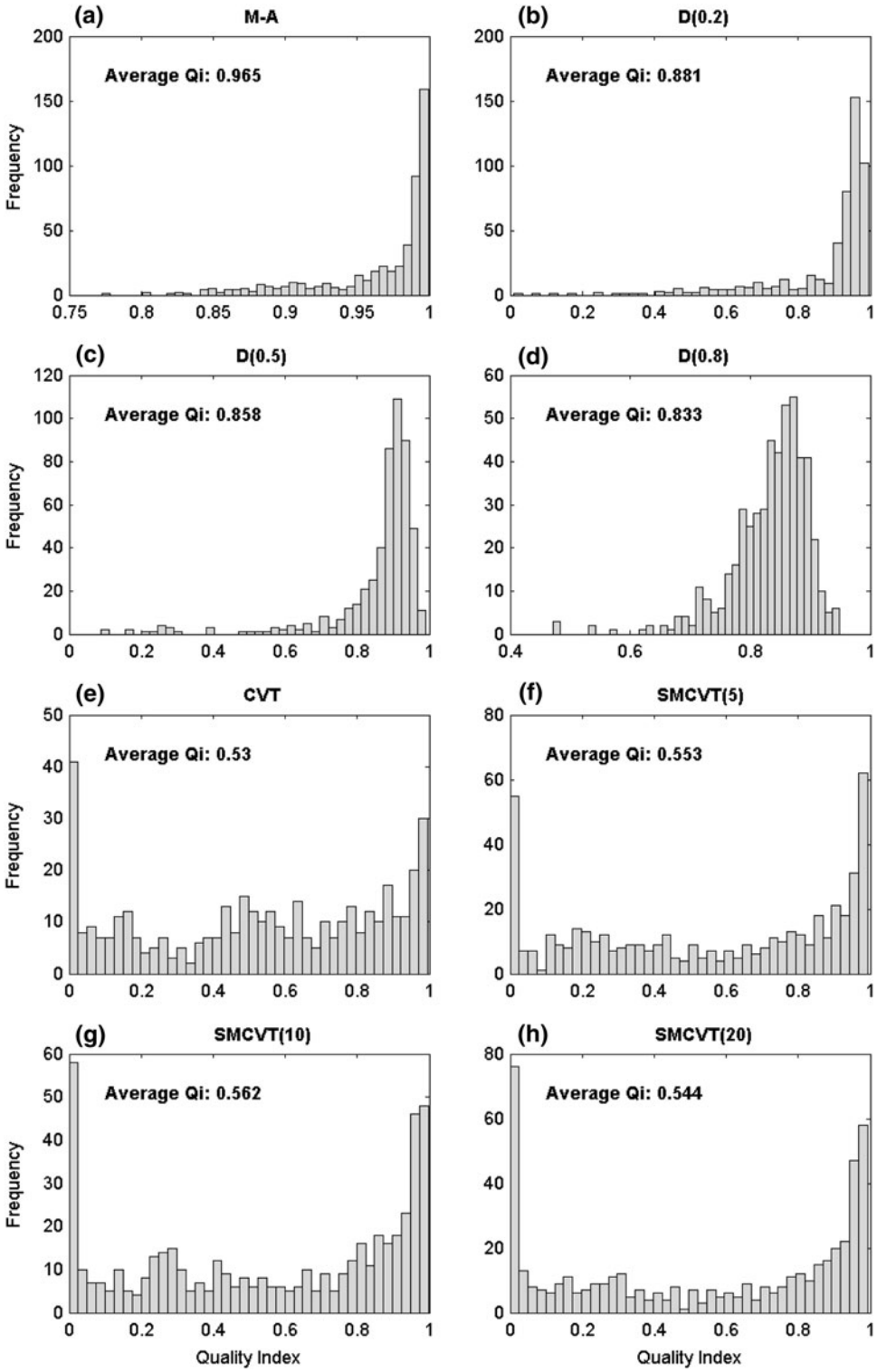

Fig. 7 Histograms of QI using **a** the maximum angle method (M-A) on original profiles, the difference method (D) on original profiles with thresholds of **b** 0.2°C, **c** 0.5°C, **d** 0.8°C, and the curvature method (CVT) on profiles after **e** no, **f** 5 times, **g** 10 times, **h** 20 times 5-point smoothing (SMCVT)

5 Comparison between maximum angle and curvature methods

Both the maximum angle and curvature methods are objective. The major difference is data fitting, i.e., Eq. (2), used in the maximum angle method and second derivatives used in the curvature method. The second-order derivatives of $T(z_k)$ versus depth are computed by a non-homogeneous mesh difference scheme,

$$\frac{\partial^2 T}{\partial z^2}\Big|_{z_k} \approx \frac{1}{z_{k+1} - z_{k-1}}\left(\frac{T_{k+1} - T_k}{z_{k+1} - z_k} - \frac{T_k - T_{k-1}}{z_k - z_{k-1}}\right), \tag{7}$$

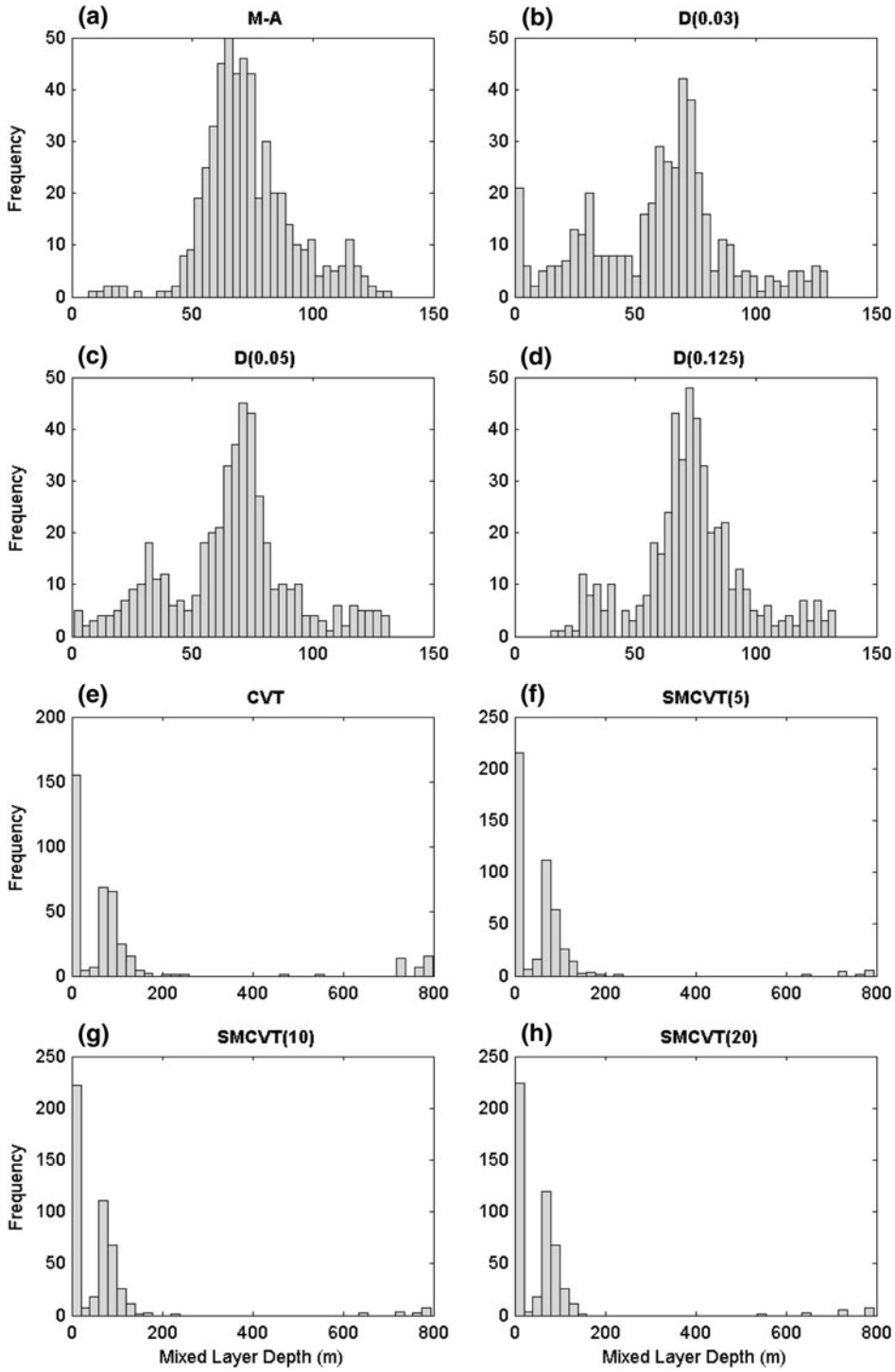

Fig. 8 Histograms of H_D identified using **a** the maximum angle method (M-A) on original profiles, the difference method (D) on original profiles with thresholds of **b** 0.03 kg/m^3, **c** 0.05 kg/m^3, **d** 0.125 kg/m^3, and the curvature method (CVT) on profiles after **e** no, **f** 5 times, **g** 10 times, **h** 20 times 5-point smoothing (SMCVT)

Table 2 Statistical characteristics of H_D identified from the two seagliders using the maximum angle, 0.03, 0.05, and 0.125 kg/m^3 thresholds

	Maximum angle	0.03 kg/m^3 threshold	0.05 kg/m^3 threshold	0.125 kg/m^3 threshold
Mean (m)	73.2	53.3	59.3	68.0
Median (m)	70.4	60.9	66.2	71.6
Standard deviation (m)	19.1	32.9	31.0	28.4
Skewness	0.28	−0.06	−0.24	−0.59
Kurtosis	4.32	2.37	2.74	3.67

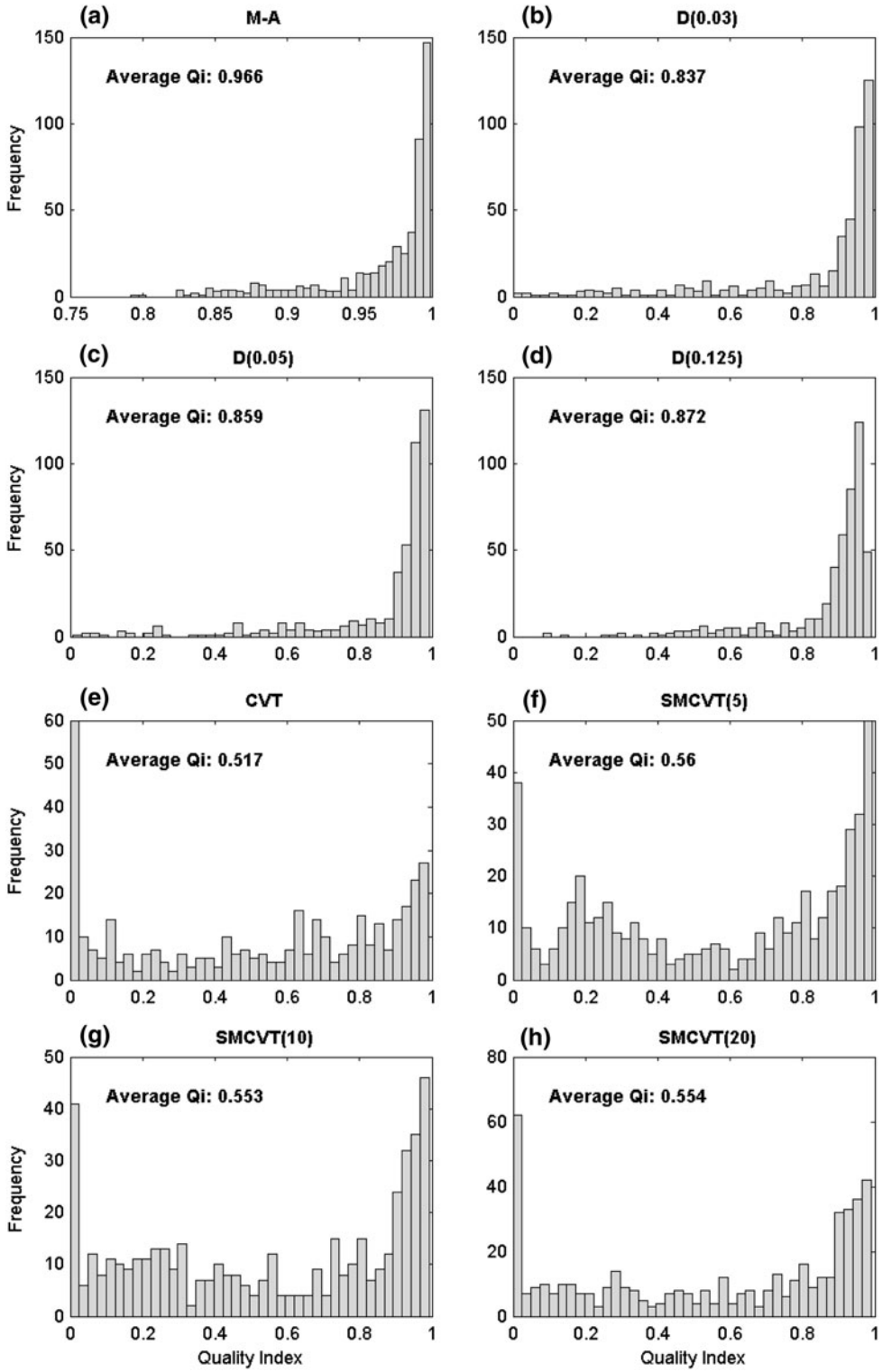

Fig. 9 Histograms of QI using **a** the maximum angle method (M-A) on original profiles, the difference method (D) on original profiles with thresholds of **b** 0.03 kg/m^3, **c** 0.05 kg/m^3, **d** 0.125 kg/m^3, and the curvature method (CVT) on profiles after **e** no, **f** 5 times, **g** 10 times, **h** 20 times 5-point smoothing (SMCVT)

where $k = 1$ refers to the surface, with increasing values indicating downward extension of the measurement. Equation 7 shows that we need two neighboring values, T_{k-1} and T_{k+1}, to compute the second-order derivative at z_k. For noisy profiles $\{T_k\}$ and $\{\rho_k\}$ with high vertical resolution such as the seaglider, the data fitting is robust but not the second derivative. Before calculating the second derivative, Eq. (7), from data, the profile usually needs to be smoothed such as by 5-point moving average to remove the sharp change of the gradient. Four sets of isothermal depth were obtained from 514 temperature profiles using the curvature method with no smoothing and with 5 times, 10

times, and 20 times 5-point moving average. Figure 6e–h show histograms of 514 H_T values for the four cases by the curvature method. The isothermal depths occur mostly within 5 m, which is obviously not correct. This is caused by creation of false minimum curvature (maximum second derivative) generated by the second-derivative calculation. The histograms of 514 QI values are low for all the four cases using the curvature method (Fig. 7e–h). The mean QI values for the curvature method are 0.517 with no smoothing (Fig. 7e), 0.560 with 5 times smoothing (Fig. 7f), 0.553 with 10 times smoothing (Fig. 7g), and 0.554 with 20 times smoothing (Fig. 7h). Obviously, the curvature method is not valid to identify isothermal depth from this dataset. Similar results were obtained for the constant-density depth (see Figs. 8e–h, 9e–h).

To illustrate different performance in handling noisy data between the maximum angle and curvature methods, an analytical temperature profile with H_T of 20 m is constructed

$$T(z)=\begin{cases}21^{\circ}\mathrm{C}, & -20\,\mathrm{m}<z\le 0\,\mathrm{m}\\ 21^{\circ}\mathrm{C}+0.25^{\circ}\mathrm{C}\times(z+20\mathrm{m}), & -40\,\mathrm{m}<z\le -20\,\mathrm{m}\\ 7^{\circ}\mathrm{C}+9^{\circ}\mathrm{C}\times\exp\left(\frac{z+40\mathrm{m}}{50\mathrm{m}}\right), & -100\,\mathrm{m}\le z\le -40\,\mathrm{m}.\end{cases} \tag{8}$$

This profile was discretized with vertical resolution of 1 m from the surface to 10-m depth and of 5 m below 10-m

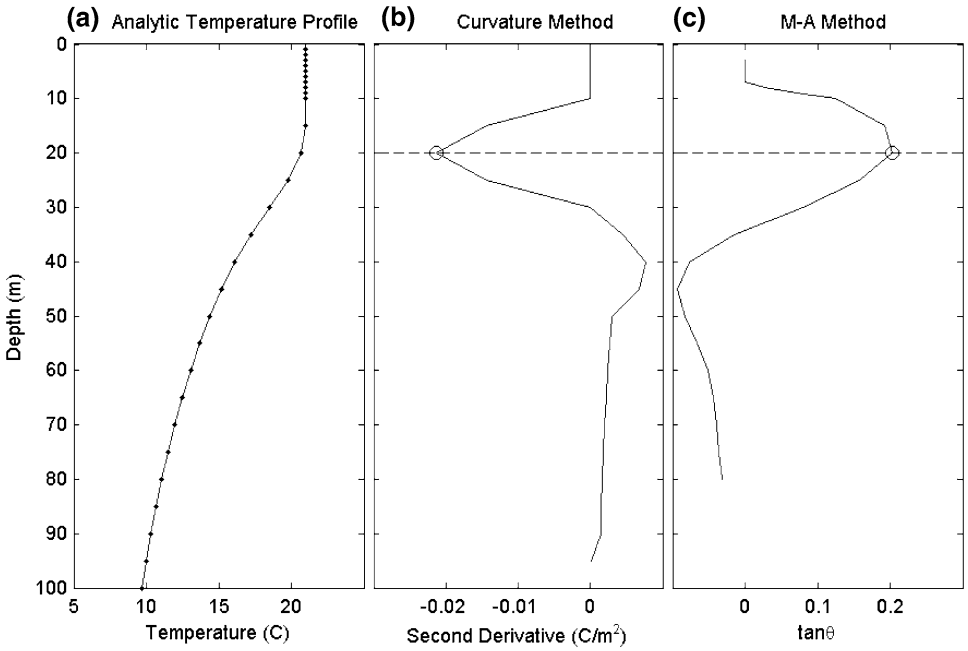

Fig. 10 **a** Smoothed analytic temperature profile, Eq. (6), by 5-point moving average, **b** calculated $(\partial^2 T/\partial z^2)_k$, and **c** (tan $\theta)_k$ from the profile data (Fig. 10a). At 20-m depth, $(\partial^2 T/\partial z^2)_k$ has a minimum value, and (tan $\theta)_k$ has a maximum value

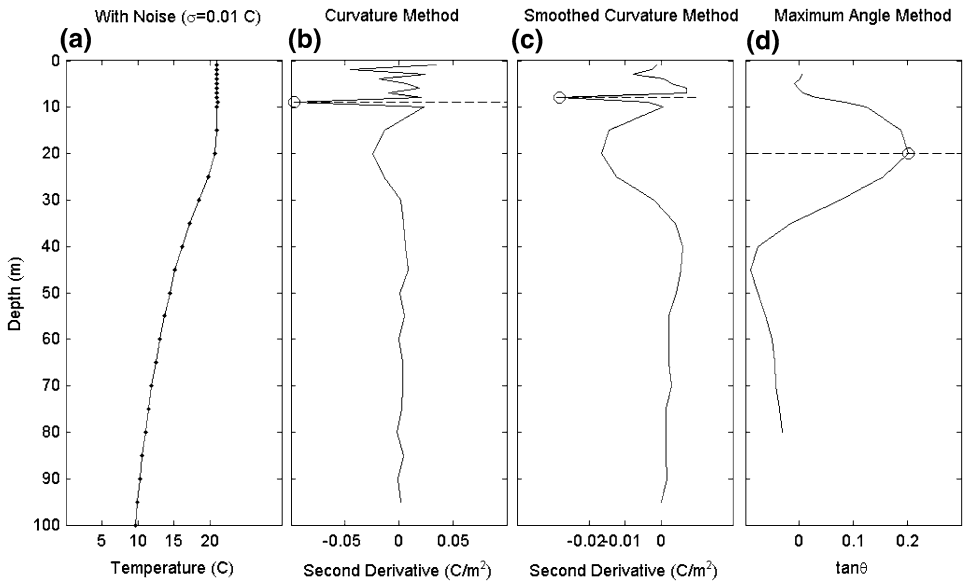

Fig. 11 One out of 1000 realizations: **a** temperature profile shown in Fig. 10a contaminated by random noise with mean of zero and standard deviation of 0.02°C, **b** calculated $(\partial^2 T/\partial z^2)_k$ from the profile data (Fig. 8a) without smoothing, **c** calculated $(\partial^2 T/\partial z^2)_k$ from the smoothed profile data (Fig. 8a) with 5-point moving average, and **d** calculated (tan $\theta)_k$ from the profile data (Fig. 8a) without smoothing

depth. The discrete profile was smoothed by 5-point moving average to remove the sharp change of the gradient at 20- and 40-m depths. The smoothed profile data [$T(z_k)$] is shown in Fig. 10a. For the surface and 100-m depth, we use the next point value, that is,

$$\frac{\partial^2 T}{\partial z^2}|_{z=0} = \frac{\partial^2 T}{\partial z^2}|_{z=-1\,\mathrm{m}}, \quad \frac{\partial^2 T}{\partial z^2}|_{z=-100\,\mathrm{m}} = \frac{\partial^2 T}{\partial z^2}|_{z=-95\,\mathrm{m}}. \tag{9}$$

Figure 10b shows the calculated second-order derivatives from the profile data listed in Table 1. Similarly, tan θ_k is calculated using Eq. (4) for the same data profile (Fig. 10c). For the profile data without noise, both the curvature method (i.e., depth with minimum $\partial^2 T/\partial z^2$, see Fig. 10b) and the maximum angle method [i.e., depth with max (tan θ), see Fig. 10c)] identified the isothermal depth, i.e., $H_T = 20$ m.

One thousand 'contaminated' temperature profiles are generated by adding random noise with mean of zero and standard deviation of 0.02°C (generated by MATLAB) to the original profile data at each depth. An example profile is shown in Fig. 11a, as well as the second-order derivative ($\partial^2 T/\partial z^2$) and tan θ. Because the random error is so small (zero mean, 0.02°C standard deviation, within the instrument's accuracy), we may not detect the difference between Figs. 10a and 11a by eye. However, the isothermal depth is 9 m (error of 11 m) using the curvature method (Fig. 11b) and 20 m (Fig. 11d) using the maximum angle method.

Usually, the curvature method requires smoothing for noisy data (Chu 1993; Lorbacher et al. 2006). To evaluate the usefulness of smoothing, a 5-point moving average was applied to the 1000 "contaminated" profile data. The second derivatives were again calculated for the smoothed profiles. The isothermal depth identified for the smoothed example profile is 8 m (Fig. 11c). Performance of the curvature method (with and without smoothing) and the maximum angle method is evaluated with the relative root-mean-square error (RRMSE),

$$\mathrm{RRMSE} = \frac{1}{H_T^{ac}}\sqrt{\frac{1}{N}\sum_{i=1}^{N}\left(H_T^{(i)} - H_T^{ac}\right)^2}, \tag{10}$$

where H_T^{ac} (=20 m) is for the original temperature profile (Fig. 10a); N (=1000) is the number of "contaminated" profiles; and $H_T^{(i)}$ is the calculated value for the ith profile. Table 3 shows the frequency distributions and the RRMSEs of the calculated isothermal depths from the "contaminated" profile data using the curvature method (without and with 5 point-moving average) and the maximum angle method without smoothing. Without 5-point moving average, the curvature method identified only 6 profiles (out of 1000 profiles) with H_T of 20 m, and the remaining profiles have H_T ranging from 1 to 10 m. The RRMSE is 76%. With 5-point moving average, the curvature method identified 413 profiles with H_T of 20 m, 164 profiles with H_T of 15 m, 3 profiles with H_T of 10 m, and the rest with H_T ranging from 2 to 8 m. The RRMSE is 50%. However, without 5-point moving average, the maximum angle method identified 987 profiles with H_T of 20 m, and 13 profiles with H_T of 15 m. The RRMSE is less than 3%.

Table 3 Frequency distributions and RRMSE of calculated isothermal depths from the data consisting of the profile (indicated in Table 1) and random noise with mean of 0 and standard deviation of 0.02°C using the curvature method (without and with 5 point-moving average) and the maximum angle method without smoothing

Isothermal layer depth (m)	Frequency: curvature (without smoothing)	Frequency: curvature (with smoothing)	Frequency maximum angle (without smoothing)
1	103	0	0
2	125	83	0
3	103	55	0
4	126	44	0
5	98	52	0
6	95	47	0
7	121	43	0
8	105	96	0
9	118	0	0
10	0	3	0
15	0	164	13
20	6	413	987
Total	1000	1000	1000
RRMSE (%)	76	50	<3

The total number of contaminated data profiles is 1000

6 Existence of barrier layer

With H_D and H_T, the BLT is easily calculated from all 514 profiles. BLT is plotted versus time in Fig. 12a (Seaglider-A) and Fig. 12b (Seaglider-B) using the maximum angle method. These two figures reveal the rather frequent occurrence of a barrier layer in the western North Atlantic. For example, among 265 stations from Seaglider-A, 66.4% (176 profiles) recorded barrier layers. The BLT has a maximum value of 30.0 m on 30 November 2007. Among 249 stations from Seaglider-B, the barrier layer occurs in 131 stations (52.6%).

From Tables 1 and 2, the mean values of H_T and H_D are 77.2 and 73.2 m, the mean BLT found by the maximum angle method is 4.0 m. When the difference method is used, the BLT depends on the threshold. For example, de Boyer Montegut et al. (2004) used 0.2°C and 0.03 kg/m^3.

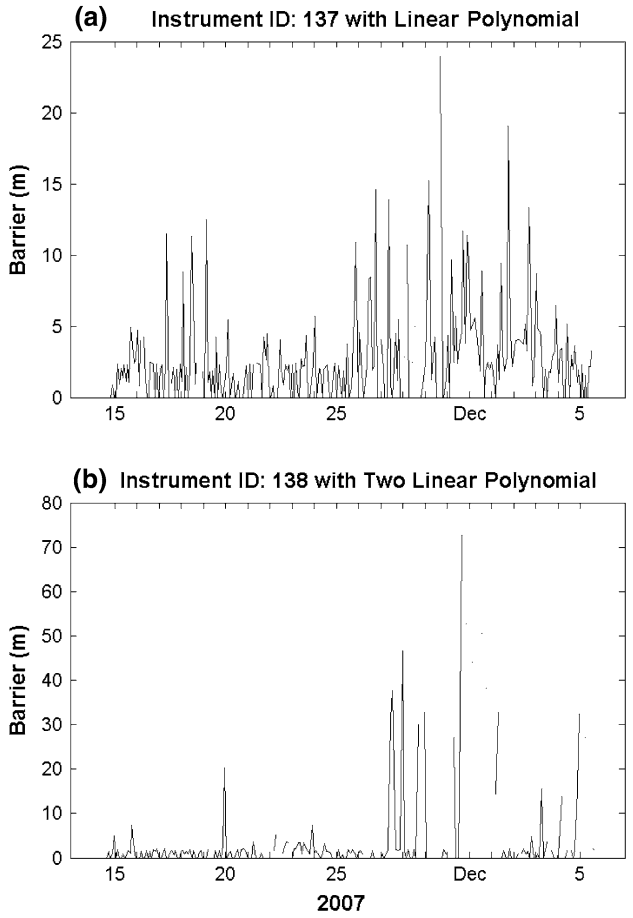

Fig. 12 Temporally varying barrier layer depth identified by the maximum angle method from: **a** Glider-A and **b** Glider-B

From Tables 1 and 2, the mean values of H_T and H_D are 71.9 and 53.3 m, which lead to the mean BLT of 18.6 m. Monterey and Levitus (1997) used 0.5°C and 0.125 kg/m^3. From Tables 1 and 2, the mean values of H_T and H_D are 82.0 and 68.0 m, which lead to the mean BLT of 14.0 m. Threshold methods find fewer but larger barrier layers than the maximum angle method.

7 Conclusions

A new maximum angle method is proposed in this study to identify isothermal and constant-density layer depths. First, two vectors (both pointing downward) are obtained using linear fitting. Then, the tangent of the angle (tan θ) between the two vectors is calculated for all depth levels. Next, the isothermal (or constant-density) depth which corresponds to the maximum value of tan θ is found. Two features make this method attractive: (1) it is less subjective than threshold methods and (2) it is able to process noisy data. The temperature and potential density profiles collected from two seagliders in the Gulf Stream near the Florida coast during 14 November–5 December 2007 were used to evaluate the new algorithm. With high quality indices (QI $\sim$ 96%), the maximum angle method not only identifies H_D and H_T, but also the gradients [$G^{(2)}$] beneath the mixed layer. One weakness of the maximum angle method is its dependence on linear regressions, which might make the method unsuitable for low-resolution profiles. Therefore, application of this method to the worldwide temperature and density profiles needs further evaluation.

Acknowledgments The Naval Oceanographic Office (document number N6230609PO00123) supported this study. The authors thank the Naval Oceanographic Office for providing hydrographic data from two seagliders.

References

Brainerd KE, Gregg MC (1995) Surface mixed and mixing layer depths. Deep Sea Res Part A 9:1521–1543

Chu PC (1993) Generation of low frequency unstable modes in a coupled equatorial troposphere and ocean mixed layer. J Atmos Sci 50:731–749

Chu PC, Fan CW (2010) Optimal linear fitting for objective determination of ocean mixed layer depth from glider profiles. J Atmos Ocean Technol 27:1893–1898

Chu PC, Fralick CR, Haeger SD, Carron MJ (1997) A parametric model for Yellow Sea thermal variability. J Geophys Res 102:10499–10508

Chu PC, Wang QQ, Bourke RH (1999) A geometric model for Beaufort/Chukchi Sea thermohaline structure. J Atmos Ocean Technol 16:613–632

Chu PC, Fan CW, Liu WT (2000) Determination of sub-surface thermal structure from sea surface temperature. J Atmos Ocean Technol 17:971–979

Chu PC, Liu QY, Jia YL, Fan CW (2002) Evidence of barrier layer in the Sulu and Celebes Seas. J Phys Oceanogr 32:3299–3309

de Boyer Montegut C, Madec G, Fischer AS, Lazar A, Iudicone D (2004) Mixed layer depth over the global ocean: an examination of profile data and a profile-based climatology. J Geophys Res 109:C12003. doi:10.1029/2004JC002378

Kara AB, Rochford PA, Hurlburt HE (2000) Mixed layer depth variability and barrier layer formation over the North Pacific Ocean. J Geophys Res 105:16783–16801

Lorbacher K, Dommenget D, Niiler PP, Kohl A (2006) Ocean mixed layer depth: a subsurface proxy of ocean-atmosphere variability. J Geophys Res 111:C07010. doi:10.1029/2003JC002157

Mahoney KL, Grembowicz K, Bricker B, Crossland S, Bryant D, Torres M (2009) RIMPAC 08: Naval Oceanographic Office glider operations. Proc SPIE 7317:731706. doi:10.1117/12.820492

Monterey G, Levitus S (1997) Seasonal variability of mixed layer depth for the world ocean. NOAA Atlas NESDIS 14, Natl. Oceanic and Atmos. Admin., Silver Spring, MD

Suga T, Motoki K, Aoki Y, Macdonald AM (2004) The North Pacific climatology of winter mixed layer and mode waters. J Phys Oceanogr 34:3–22

Wyrtki K (1964) The thermal structure of the eastern Pacific Ocean. Dstch Hydrogr Zeit Suppl Ser A 8:6–84